ChemComm

Chemical Communications

www.rsc.org/chemcomm

Number 21 | 7 June 2008 | Pages 2393–2484

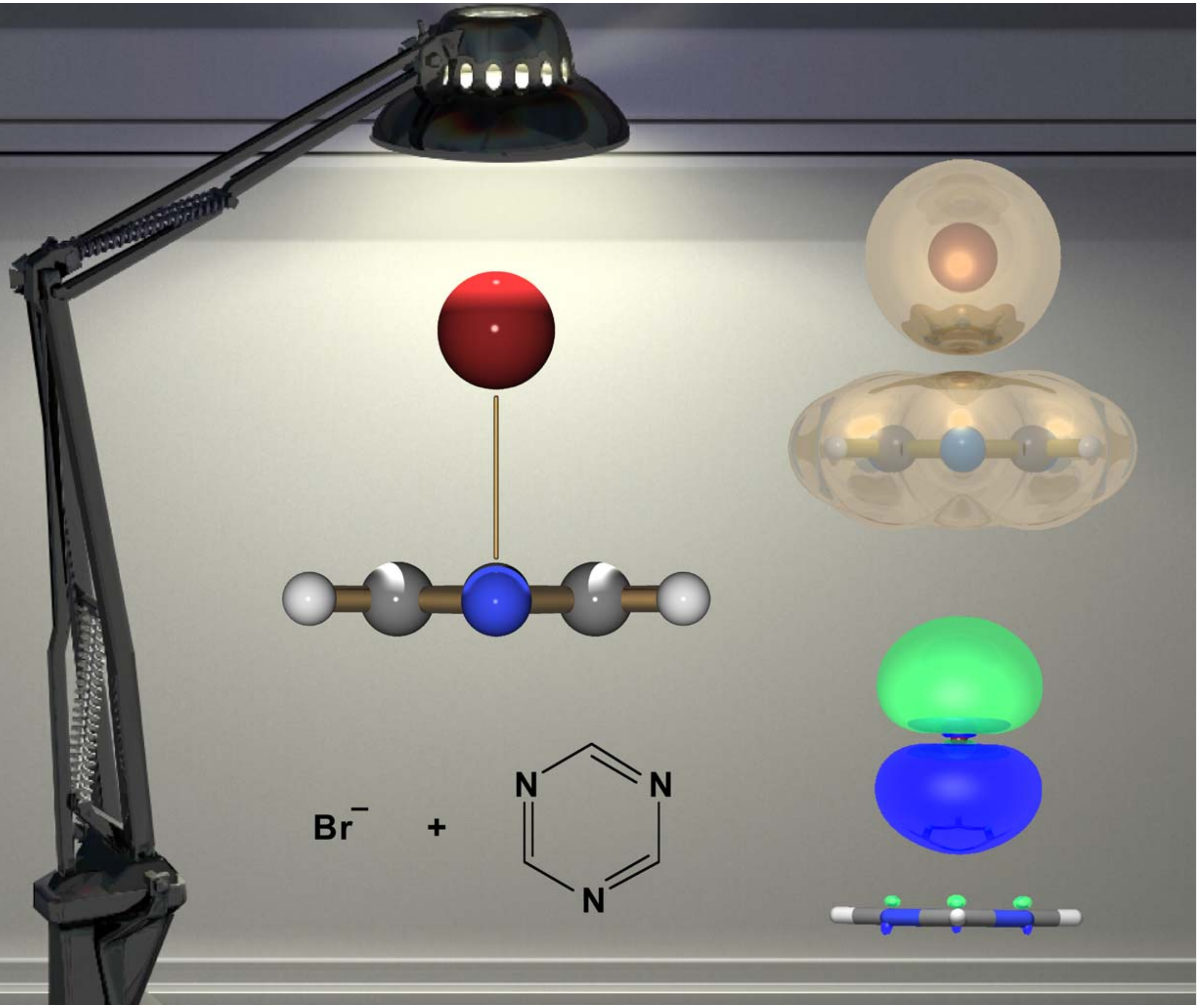

ISSN 1359-7345

FEATURE ARTICLE
Benjamin P. Hay and Vyacheslav S. Bryantsev
Anion–arene adducts: C–H hydrogen bonding, anion–π interaction, and carbon bonding motifs

RSC Publishing

Anion–arene adducts: C–H hydrogen bonding, anion–π interaction, and carbon bonding motifs†

Benjamin P. Hay*[a] **and Vyacheslav S. Bryantsev**[b]

Received (in Cambridge, UK) 3rd January 2008, Accepted 15th January 2008
First published as an Advance Article on the web 4th March 2008
DOI: 10.1039/b800055g

This article summarizes experimental and theoretical evidence for the existence of four distinct binding modes for complexes of anions with charge-neutral arenes. These include C–H hydrogen bonding and three motifs involving the arene–π system—the noncovalent anion–π interaction, weakly covalent σ interaction, and strongly covalent σ interaction.

Introduction

"There is nothing new under the sun, but there are a lot of old things we don't know." – Ambrose Bierce (1842–1914)

The interaction of anions with arenes has been studied for over a century. Colored solutions observed when anions were added to solutions containing electron-deficient aromatics initiated extensive studies of charge-transfer complexes[1] and intermediates involved in nucleophilic aromatic substitution reactions.[2] In the 1980s, application of high pressure mass spectrometry methods allowed gas-phase characterization of ion–molecule complexes, which when coupled with Hartree–Fock calculations, yielded further insight into the nature of anion–arene interactions.[3] Renewed interest in this topic surfaced with the expanding study of supramolecular chemistry pertaining to anions.[4]

Over the past decade anion complexation by synthetic host molecules has become an important theme in supramolecular chemistry.[5] A key challenge is the development of hosts that exhibit anion recognition. A variety of reversible binding interactions are being explored to address this challenge, such as hydrogen bonding, electrostatic interactions, and metal ion coordination. Understanding the geometric and energetic aspects of individual binding interactions, one focus of our research,[6] provides the basis for the deliberate design of host architectures that are tailored for specific guests.[7]

As this review will establish, arenes, in particular electron-deficient arenes, form a variety of quite stable, reversible complexes with anions. Thus, arenes are viable binding sites in anion receptor design. Although recent literature has focused almost exclusively on the anion–π interaction,[8] it has been recognized for some time that multiple arene bonding motifs are possible.[3] Other motifs include aryl C–H hydrogen bonding and covalent interactions with aryl carbons. In the brief space allotted here, we (i) summarize what is known about the various ways that simple anions, such as halides, nitrate, and perchlorate, may interact with charge-neutral arenes, (ii) suggest new criteria for distinguishing between different bonding motifs, and (iii) propose usage of nomenclature to avoid further confusion in the literature. Due to space limitations, related studies involving arenes that are bound to metal cations[9] and positively charged arenes[10] are intentionally excluded from this discussion.

C–H hydrogen bonding interactions

Although it is well established that C–H groups can serve as hydrogen bond donors, it is generally believed that C–H

Benjamin P. Hay

B.Sc. Chemistry, U Missouri-Columbia, 1980; Ph.D. Chemistry, U Oregon with Prof. R. G. Finke, 1986; Aust Natl U-Canberra with Prof. A. L. J. Beckwith, 1987–88; Los Alamos Natl Lab with Dr G. D. Jarvinen, 1989–90; Research Scientist, Pacific NW Natl Lab, 1991–2006; Distinguished Scientist, Oak Ridge Natl Lab, 2006–date. Interests: computer-aided molecular design, supramolecular chemistry.

Vyacheslav S. Bryantsev

B.Sc. Chemistry, Donetsk State U, 1999; Ph.D. Chemistry, Natl Acad Science Ukraine with Prof. Y. B. Vysotsky, 2003; Pacific NW Natl Lab with Dr B. P. Hay, 2004–06; Research Scientist, Materials and Process Information Center, Cal Inst Tech with Prof. W. A. Goddard III, 2006–date. Interests: electronic structure theory, structure-based molecular design, and solvation models.

---

[a] Chemical Sciences Division, Oak Ridge National Laboratory, PO Box 2008, Oak Ridge, TN 37831-6119, USA. E-mail: haybp@ornl.gov; Fax: +1 865-574-4939; Tel: +1 865-574-6717
[b] Materials and Process Simulation Center (139-74), Division of Chemistry and Chemical Engineering, California Institute of Technology, 1200 East California Blvd., Pasadena, CA 91125, USA. E-mail: slava@wag.caltech.edu; Fax: +1 626-585-0918; Tel: +1 626-395-8138

† Electronic supplementary information (ESI) available: Cartesian coordinates and absolute energies for the C_{3v} and C_1 forms of the TAZ–NO_3^- adducts. See DOI: 10.1039/b800055g

groups form much weaker hydrogen bonds than conventional donor groups such as O–H and N–H. Indeed, there is a book entitled 'The Weak Hydrogen Bond in Structural Chemistry and Biology' that focuses largely on the interactions of C–H donor groups with neutral oxygen and nitrogen acceptor atoms.[11] Evidence for the weak nature of these interactions comes from structural, spectrosopic, and theoretical data. With respect to the latter, gas phase binding energies, ΔE, obtained from electronic structure calculations provide a quantitative scale to assess the relative strengths of hydrogen bonding interactions in the absence of complicating effects present in condensed phases. Evaluation of the ΔE value allows one to classify hydrogen bonds as weak, <17 kJ mol^{-1}, moderate, 17 to 63 kJ mol^{-1}, and strong, >63 kJ mol^{-1}.[12]

Calculated ΔE values for simple alkane and arene C–H donors with neutral oxygen acceptors, such as water or formaldehyde, range from -1.3 kJ mol^{-1} for CH_4 to -5.7 kJ mol^{-1} for the more acidic hydrogens in benzene.[13] These interactions fall within the weak category and certainly are weak when compared with conventional hydrogen bonds, such as the O–H···O interaction in the water dimer, -20.9 kJ mol^{-1},[14] or the N–H···O interaction in the acetamide–water complex, -29.3 kJ mol^{-1}.[15] Given this precedent, one might reason that contacts observed between aryl C–H donors and anion acceptors should be classified as weak hydrogen bonds and thus should not play a significant role in anion coordination chemistry. It turns out, however, that this is not the case.

Some of the earliest evidence regarding aryl C–H hydrogen bonding comes from the mass spectrometric evaluation of ion–molecule equilibria where it was observed that Cl^- formed stable complexes with a variety of arenes, including benzene itself.[16] On the basis of HF/STO-3G calculations, it was concluded that these complexes involved C–H···Cl hydrogen bonding. Two possible geometries for the benzene complex were identified: linear with a single hydrogen bond and bifurcated with two hydrogen bonds (see Fig. 1). Subsequent experiments yielded enthalpies of formation for the benzene–Cl^- complex of –41.4 kJ mol^{-1} and –39.3 kJ mol^{-1},[17,18] establishing these hydrogen bonds to be of moderate strength.

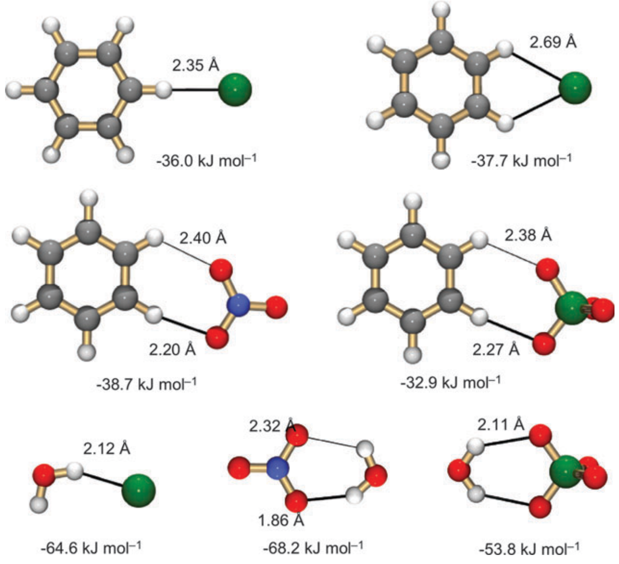

Fig. 1 Geometries and ΔE values for complexes of Cl^-, NO_3^-, and ClO_4^- with benzene and water (MP2/aug-cc-pVTZ single-point energies on MP2/aug-cc-pVDZ geometries).[20]

More recent high-level electronic structure calculations fully support these earlier results. In studies of benzene–halide complexes, MP2/aug-cc-pVDZ optimizations corroborate the existence of both linear and bifurcated minima, with the latter form being slightly more stable for Cl^- through I^-.[19] In Fig. 1, calculated geometries and ΔE values for stable benzene complexes with spherical Cl^-, trigonal planar NO_3^-, and tetrahedral ClO_4^- anions are compared with results obtained for corresponding anion–water complexes.[20] With ΔE values ranging from -32 to -39 kJ mol^{-1}, the calculated results confirm that benzene C–H groups form hydrogen bonds of moderate strength with these univalent anions. To place these results in perspective, the C–H donor groups in these benzene complexes yield hydrogen bonds that are roughly 60% the strength of those formed by the O–H donor groups in the corresponding water complexes.

The strength of an aryl C–H donor group can be tuned by adding functional groups to the arene ring. Early mass spectrometric studies established that it was possible to more than double the strength of the aryl C–H hydrogen bond in this manner.[3,16] In the case of Cl^- and Br^-, plots of the gas phase free energy of complex formation *versus* Taft substituent parameters yielded linear correlations for series of monosubstituted benzenes. Theoretical calculations yield analogous results for complexes of monosubstituted benzenes with Cl^- and NO_3^-, where computed ΔE values, Table 1, also yield linear correlations when plotted against Taft substituent constants.[21] Electron-withdrawing groups strengthen the interaction and electron-donating groups weaken the interaction. Strong electron-withdrawing groups, CN and NO_2, yield strong hydrogen bonds with ΔE values ranging from -65 to -70 kJ mol^{-1}. Multiple substitution with electron-withdrawing substituents can result in very strong hydrogen bonding

Table 1 Influence of substituent, X, on electronic binding energies, ΔE, (kJ mol^{-1})[a]

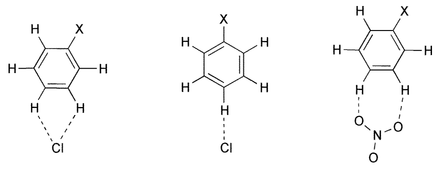

X	ΔE	ΔE	ΔE
NH_2	−31.5	−29.4	−32.6
CH_3	−35.1	−33.3	−36.2
H	−37.7	−36.0	−38.7
Cl	−52.1	−49.3	−52.1
CF_3	−59.3	−56.7	−59.3
CN	−68.6	−65.3	−67.8
NO_2	−70.1	−67.1	−69.5

[a] MP2/aug-cc-pVTZ single-point energies on MP2/aug-cc-pVDZ optimized geometries.[21]

Table 2 Aryl C–H contact distances observed in the CSD[a]

Anion	C–H···X/Å	C···X/Å	n_{obs}
Cl^-, linear	2.77 ± 0.15	3.81 ± 0.15	1471
Cl^-, bifurcated	3.07 ± 0.15	3.82 ± 0.15	288
Br^-, linear	2.96 ± 0.20	4.00 ± 0.20	808
Br^-, bifurcated	3.19 ± 0.17	3.94 ± 0.16	180
I^-, linear	3.14 ± 0.16	4.16 ± 0.16	532
I^-, bifurcated	3.39 ± 0.19	4.13 ± 0.17	229
NO_3^-	2.57 ± 0.20	3.60 ± 0.19	849
ClO_4^-	2.60 ± 0.19	3.63 ± 0.19	2798
SO_4^{2-}	2.49 ± 0.17	3.53 ± 0.16	46

[a] Table reports the mean and standard deviation, σ, for distances and the number of observations within $\pm 3\sigma$ of the mean C–H···X distance, n_{obs}, where X is the anion atom involved in the hydrogen bond. CSD search criteria are summarized in Fig. 2 caption.

interactions. For example, 1,3,5-tricyanobenzene and 1,2,4,5-tetracyanobenzene form C–H hydrogen bonds with Cl^- that exhibit ΔE values of −90.5 and −113.0 kJ mol^{-1}, respectively.[22]

Thus, both experiment and theory establish that aryl C–H groups form moderate to strong hydrogen bonds with anions, suggesting that these interactions should play an important role in supramolecular chemistry. Searches of the Cambridge Structural Database (CSD)[23] for aryl C–H···anion contacts between substituted benzene rings and common anions reveal that such interactions are very common in the solid state.

Searches for aryl C–H contacts with Cl^- yielded 1471 examples of the linear geometry (C–H···Cl angle ≥ 150°) and 288 examples of the bifurcated geometry (120° ≤ C–H···Cl angles ≤150°). These examples include cases where benzene is the C–H donor (Fig. 1) for both linear[24] and bifurcated[25] Cl^- complexes. Similar searches conducted for Br^- and I^-, as well as oxoanions NO_3^-, ClO_4^-, and SO_4^{2-} (one C–H···O angle ≥ 150°) located many more examples (see Table 2).

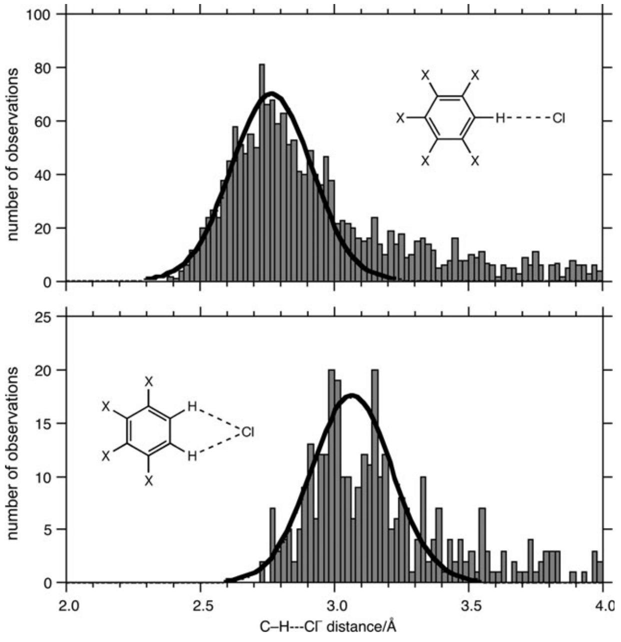

Fig. 2 Histograms of aryl C–H···Cl^- distances observed in the CSD for linear (top) and bifurcated (bottom) hydrogen bonding motifs, X = any atom. Gaussian fits are shown by the solid curves. Search criteria: r_{fac} ≤0.10, no error, no disorder, C–H distances normalized to 1.083 Å; linear motif, C–H···Cl angle ≥ 150°; bifurcated motif, both C–H···Cl angles ≥ 120° and ≤150°.

Geometric parameters obtained from the crystal structure data can be compared with structures calculated in isolation. The main difference between the two is that the intermolecular distances in the calculated structures are generally shorter than those observed in crystal structures. For example, histograms for the C–H···Cl^- distance distributions, Fig. 2, yield mean values of 2.77 Å for the linear form and 3.07 Å for the bifurcated form, whereas the calculated values for benzene (Fig. 1) are 2.35 and 2.69 Å, respectively. Comparison of the experimental distances given in Table 2 with calculated distances given in Fig. 1 shows that the latter are on average 0.38 Å shorter than those observed in crystals. This difference is expected because (i) the single anion–molecule interaction in the calculation polarizes and redistributes the charge on the anion in a different way than the multiple anion–molecule interactions typically present in any crystalline environment and (ii) hydrogen bonds, which are predominantly electrostatic, are weakened when placed in dielectric medium.

Interactions with the arene π-system

As noted in the introduction, the interaction of anions with arene π-systems is an area that has received much recent attention. Though the majority of the attention has been focused on the noncovalent anion–π interaction, there exist alternate interaction motifs that possess varying degrees of covalent character. A year ago we presented evidence for the existence of three distinct motifs for halide interaction with the π-systems of four electron-deficient arenes.[22] These arenes, which will serve as examples below, include 1,3,5-triazine (TAZ), hexafluorobenzene (C_6F_6), 1,3,5-tricyanobenzene (3CN), and 1,2,4,5-tetracyanobenzene (4CN).

The remainder of this section is divided into four parts. Because halides represent the best characterized and, therefore, the best understood examples, halide–arene complexes are used as examples in the first three parts to define the characteristics of the three interaction types: (a) anion–π, (b) strong σ, and (c) weak σ. In the fourth part, (d), we show how methods used to characterize halide binding motifs can be extended to arene complexes with other anions.

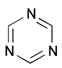

TAZ

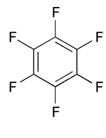

C_6F_6

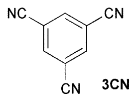

3CN

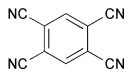

4CN

(a) Noncovalent anion–π interactions

Two decades ago gas phase studies revealed that C_6F_6 formed a strong complex with Cl^-, ΔH = −70.3 kJ mol^{-1}.[26] Further studies detected stable C_6F_6–X^- gas phase adducts, X^- = Cl^-, Br^-, and I^-, and electronic structure calculations, HF/3-21G*, revealed that these adducts resulted from a noncovalent interaction between the halide and this electron-deficient arene, with the halide perched above the arene centroid.[27]

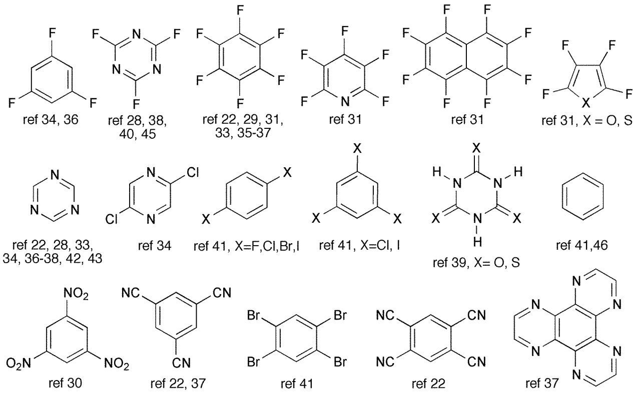

Fig. 3 Charge-neutral arenes for which theoretical anion–π complexes have been reported.

No further study was made of these interesting complexes until 2002, when there were four reports of theoretical calculations confirming a stabilizing interaction when anions are centered over the face of electron-deficient arenes such as TAZ,[28] C_6F_6,[29] trinitro- and trifluorobenzene,[30] and a variety of perfluorinated arenes.[31] In accord with nomenclature established for the noncovalent interaction between cations and benzene, the cation–π interaction,[32] this anion binding motif was termed the *anion–π interaction*.[29]

Anion–π interactions with charge-neutral arenes have been the focus of extensive theoretical study. Over the past five years 141 calculated geometries have been reported for anion–π complexes with a variety of arenes, Fig. 3.[22,28–31,33–46] On close inspection, we find these studies to be somewhat misleading. Where frequency calculations were done to establish whether reported geometries were minima (129 cases), many of the theoretical structures (56 out of the 129 cases) exhibited one or more negative frequencies and could be obtained only by the imposition of symmetry constraints. In other words, roughly half of the reported anion–π complexes are predicted not to exist in the gas phase!

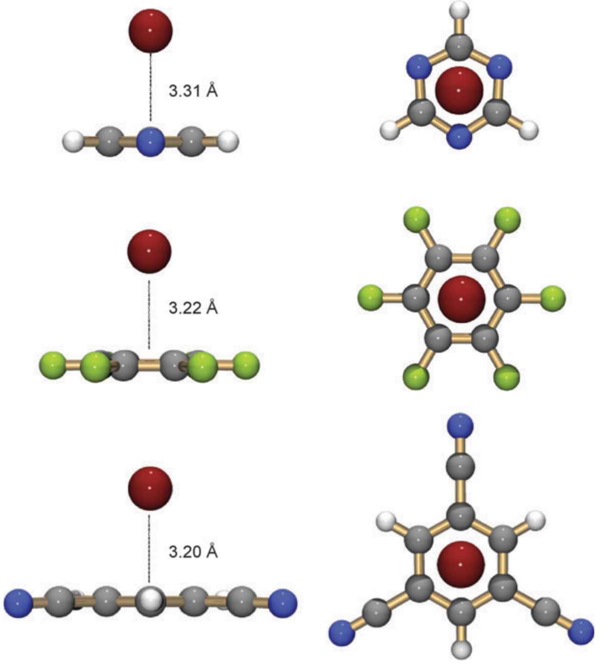

Fig. 4 Anion–π complexes for Br^- and TAZ (top), C_6F_6 (middle), and 3CN (bottom). Values for $d_{centroid}$ are provided for each structure. Geometries optimized at the MP2/aug-cc-pVDZ level of theory.[22]

Consistent with this observation, when we evaluated the twelve possible anion–π complexes formed by combining F^-, Cl^-, and Br^- anions with TAZ, C_6F_6, 3CN, and 4CN arenes, only five structures were actually minima: Cl^- with TAZ and C_6F_6, and Br^- with TAZ, C_6F_6, and 3CN.[22] Geometries for the Br^- complexes are shown in Fig. 4. Although many 1 : 1 anion–π complexes have been reported for F^-, not one of them has been a minimum. Without exception, the F^- anion adopts an alternative mode of interacting with arene carbon atoms—see part (b) below.

Anion–π complexes formed by Cl^- and Br^- are the best theoretically characterized examples for this interaction type. Results depend strongly on the level of theory applied, with HF, DFT, and MP2 yielding significantly different structures and energies.[31,35,36] Although DFT methods are attractive due to their computational efficiency, they should be used with caution as their failure to treat the dispersion forces (van der Waals interactions) present in these complexes gives rise to longer distances and weaker ΔE values than are obtained at the more accurate levels of theory. For example, in the case of the TAZ–Cl^- complex, B3LYP/6-31++G* gives $\Delta E = -17.6$ kJ mol^{-1} and $d_{centroid} = 3.475$ Å, whereas MP2/6-31++G* gives $\Delta E = -36.8$ kJ mol^{-1} and $d_{centroid} = 3.220$ Å.[36]

Calculated anion–π complexes with symmetric arenes all exhibit geometries in which the halide is located exactly above the arene centroid. This geometry is characterized by the distance from the centroid to the halide, $d_{centroid}$. For complexes that represent minima at the MP2 level of theory, reported $d_{centroid}$ values range from 3.00 to 3.25 Å for Cl^- and 3.15 to 3.40 Å for Br^-. Distances for representative Br^- complexes are given in Fig. 4. Reported ΔE values for Cl^- range from −36 to −97 kJ mol^{-1}. Reported ΔE values for Br^- range from −25 to −110 kJ mol^{-1}. For the Br^- complexes shown in Fig. 4, ΔE values are −34.9, −65.1, and −88.6 kJ mol^{-1} for TAZ, C_6F_6, and 3CN, respectively.[22]

In addition to their characteristic geometries, another defining trait of the anion–π complex is the noncovalent nature of the interaction. A variety of analyses have shown that this interaction is dominated by two components—(i) electrostatic attraction between the negative charge of the anion and the electric field of the arene and (ii) anion-induced polarization of the arene. Evidence for the lack of any appreciable covalency, in other words, of any appreciable charge transfer from the anion to the arene, has been furnished by the analysis of charge distributions,[22,27] AIM analysis,[29–31] NBO analysis,[22] and visualization of electron density isosurfaces.[22] Application of the last method is developed in further detail below.

With modern software, such as ECCE,[47] it is possible to render electron density isosurfaces using the wavefunction obtained from electronic structure calculations. Depending on the value of the density, these surfaces can serve to locate atoms, delineate covalent bonds, or indicate overall molecular size and shape.[48] By rendering the density surface at different isovalues, which have units of e Å^{-3}, it is possible to visually

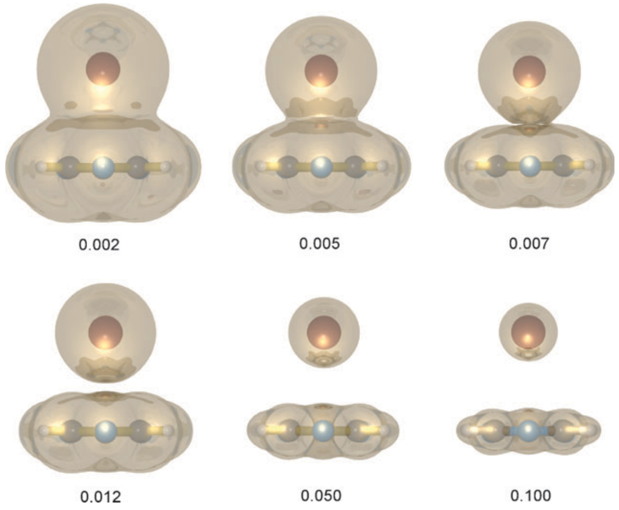

Fig. 5 Renderings of *e* density surfaces for the TAZ–Br^- anion–π complex (Fig. 4), isovalues/e $Å^{-3}$ are given beneath each structure.

determine the maximum density in the region between two bonded entities, ρ_{max}. This value, which is similar to the $\rho(r_c)$ value in AIM theory,[49] provides a quantitative measure of the degree of covalency. Bonds that are considered covalent generally have ρ_{max} values >0.1 e $Å^{-3}$.[48] At the MP2/aug-cc-pVDZ level, we obtain values for C–C bonds of 0.25 e $Å^{-3}$ in ethane, 0.35 e $Å^{-3}$ in ethene, and 0.41 e $Å^{-3}$ in ethyne. At the other end of the spectrum, noncovalent interactions exhibit much lower ρ_{max} values. For example, we find that the Ne_2 van der Waals dimer exhibits a ρ_{max} of 0.004 e $Å^{-3}$.

A series of electron density surfaces for the TAZ–Br^- complex are illustrated in Fig. 5. At isosurface values ≤ 0.007 e $Å^{-3}$, the electron density surfaces are continuous between Br^- and TAZ. At isosurface values >0.007 e $Å^{-3}$, the electron density surfaces are discontinuous between Br^- and TAZ. Thus, this complex exhibits a ρ_{max} of 0.007 e $Å^{-3}$, indicating the absence of covalent bonding between the anion and arene. Application of this method to stable anion–π complexes of Cl^- and Br^- determined in our prior study[22] reveals that ρ_{max} is <0.012 e $Å^{-3}$ in all cases.

Examination of canonical molecular orbitals, MOs, provides another way to gauge the degree of covalency in an interaction. In cases where there is significant covalent character there will be substantial mixing of orbitals on the anion with orbitals on the arene. In the absence of any covalent character, anion orbitals will remain localized on the anion and arene orbitals will remain localized on the arene. The extent of orbital mixing can be determined by examination of the coefficients in the MO vectors and can be visualized by rendering MO isosurfaces. Like electron density isosurfaces, MO isosurfaces can be scaled to any size. For all the MOs rendered herein, we chose to use a value of 0.032 (e $Å^{-3})^{1/2}$, which gives MO surfaces that fit within the van der Waals surface of the molecule.[48]

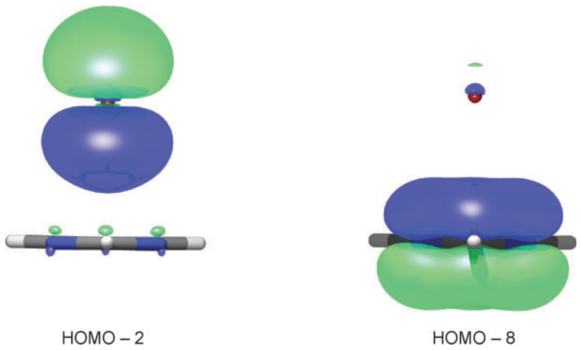

Fig. 6 Representative MOs for the TAZ–Br^- anion–π complex (Fig. 4), isovalue = 0.032 (e $Å^{-3})^{1/2}$.

Consistent with the lack of covalency indicated by the low ρ_{max} value, the MOs for the TAZ–Br^- anion–π complex reveal very little mixing of orbitals between the two species. The MOs are either predominantly localized on Br^- or on TAZ. The two MOs with the maximum mixing, based on MO vector coefficients, are shown in Fig. 6. The MO behavior in the TAZ–Br^- example is representative of other anion–π complexes with Cl^- and Br^-, in other words, there is very little mixing of halide and arene orbitals with this binding motif.

Although there is firm theoretical support for the existence of the anion–π interaction, there are surprisingly few experimental examples involving halides and charge-neutral arenes. In stark contrast to aryl C–H hydrogen bonding, where there are thousands of crystal structure examples, a thorough search of the CSD yielded only a handful of anion–π complexes.[22] In this search, a hit was defined as any halide anion located within 4.0 Å of the centroid of an electron-deficient six-membered ring in which all ring atoms were trivalent. After applying the constraint that the π-system must be charge-neutral (not conjugated with a charged species or bound to a metal cation), only 28 crystal structures remained, representing a total of 44 halide–centroid contacts. Inspection of these structures revealed (i) no examples of anion–π complexes for any of the arenes that have been studied theoretically (Fig. 3) and (ii) the majority of the contacts fail to exhibit the expected geometry for an anion–π complex.

Inspection of these crystal structures involved an analysis of the location of the halide over the face of the arene. A distance parameter, d_{offset}, was defined for this purpose (see Fig. 7). This parameter is readily obtained from distances ($d_{centroid}$ and d_{plane}) that can be queried in a CSD search. The d_{offset} value shows where the halide is located above the arene plane: 0 Å,

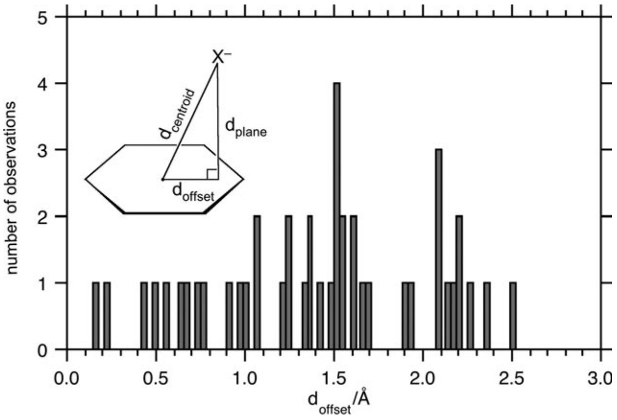

Fig. 7 Histogram of d_{offset} values for halide interactions with the π-systems of charge-neutral arenes observed in crystal structures.[22]

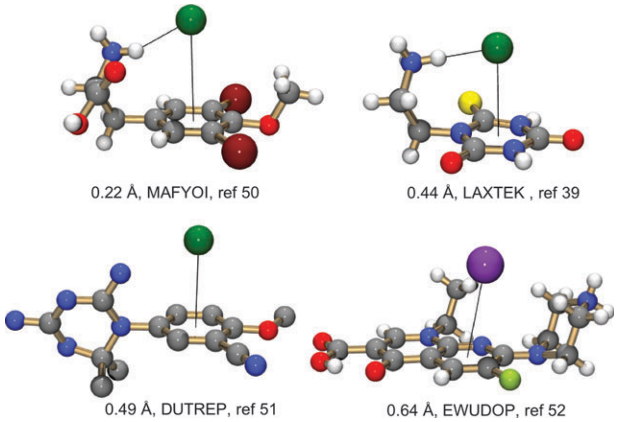

Fig. 8 Examples of anion–π complexes formed between halides and charge-neutral arenes found in the CSD. Values for d_{offset} (see Fig. 7), the CSD refcode, and reference are given below each structure.

above the centroid; 1.2 Å above a ring bond; 1.4 Å above a ring atom; ≥ 1.4 Å, outside the ring periphery. A histogram of d_{offset} values, shown in Fig. 7, reveals that only a few structures show the anion–π geometry. The distribution exhibits a maximum centered at $d_{\text{offset}} = 1.5$ Å, just outside the ring perimeter. Thus, over 80% of the halides in these structures are closer to the periphery of the π-system ($d_{\text{offset}} > 0.7$ Å) than to the centroid, suggesting the existence of an alternate binding motif (see part (c) below).

Representative examples of the halide anion–π complexes present in the CSD are shown in Fig. 8.[39,50–52] These structures all share a common feature: a cationic binding site is appended to the arene ring. A few other examples of crystal structures containing anion–π interactions between halides and charge-neutral π-systems have been reported.[39,53–55] The most recent example, a cylindrophane encapsulating F^-, exploits the same feature as the structures in Fig. 8, coupling two cyanuric acids with three cation-bearing linkages.[55]

(b) Strongly covalent σ interactions

Nucleophilic anions covalently add to electron-deficient arenes to form anionic σ complexes, also known as 'Meisenheimer' complexes. Such complexes are intermediates in the S_NAr mechanism of aromatic nucleophilic substitution[56] and have been a topic of interest since the isolation of the salt of one of these complexes in 1902.[57]

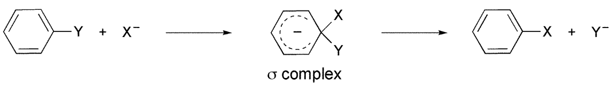

Polynitroaromatics, which represent the most extensively studied arene systems,[2] form σ complexes with a variety of nucleophilic anions including RO^-, CN^-, N_3^-, H^-, and F^-. Extensive evidence for the formation of σ complexes in solution comes from reactivity patterns as well as UV–Vis and NMR spectroscopy. Salts of a few stable σ complexes have been crystallized and a number of structures have been determined. An example is presented in Fig. 9.[58]

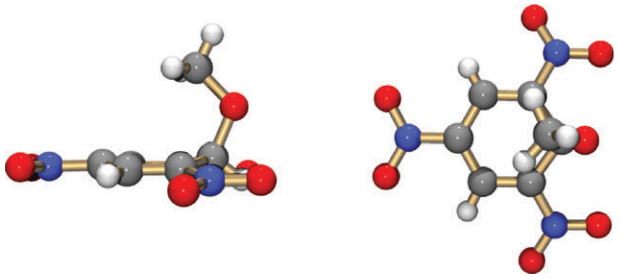

Fig. 9 Crystal structure of the σ complex formed by the addition of MeO^- to 1,3,5-trinitrobenzene, CSD refcode MXNBZK.[58]

The CSD does not contain any crystal structure examples of σ complexes in which a halide is either the attacking or leaving group. However, the most nucleophilic of the halides, F^-, has been observed to form strongly covalent σ complexes in solution.[2] All theoretical calculations of 1 : 1 arene–F^- complexes locate σ complexes, not anion–π complexes, as minima. Such results are consistent with experimental gas phase studies. For example, although C_6F_6 forms anion–π complexes with Cl^-, Br^-, and I^-,[27] it forms the much stronger σ complex with the F^- anion.[59,60] Measured gas phase ΔH values for the addition of F^- to perfluorinated arenes range from −113 to −172 kJ mol^{-1}.[60]

Results from our recent theoretical study[22] are consistent with prior reports. In all four cases, the σ complex was the only minimum that could be located in which F^- was located above the arene plane. These complexes were quite stable, exhibiting ΔE values of −109, −110, −185, and −222 kJ mol^{-1} for C_6F_6, TAZ, 3CN, and 4CN, respectively. Representative geometries, shown in Fig. 10, provide evidence for the strong covalent character of this interaction. First, the ring carbon under attack is rehybridized, exhibiting a tetrahedral, rather than trigonal planar, geometry. Second, the C–F distances are

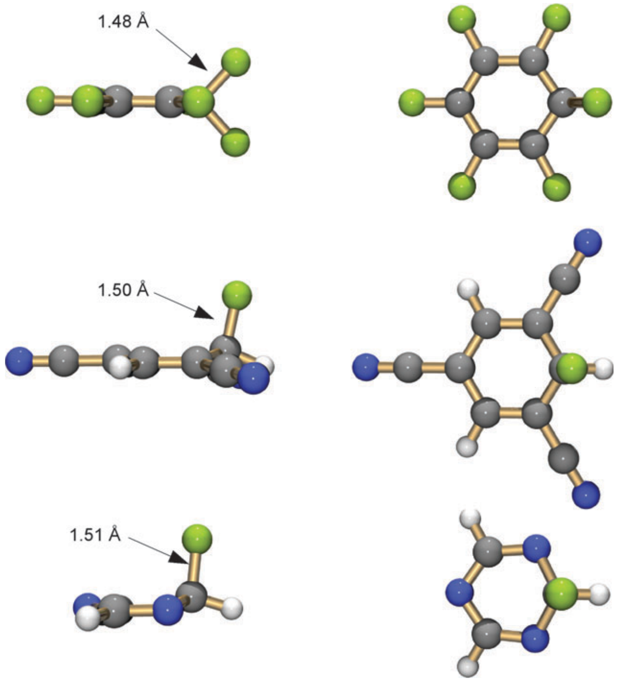

Fig. 10 Examples of strongly covalent σ complexes formed between F^- and C_6F_6 (top), 3CN (middle), and TAZ (bottom). Geometries were optimized at the MP2/aug-cc-pVDZ level of theory.[22]

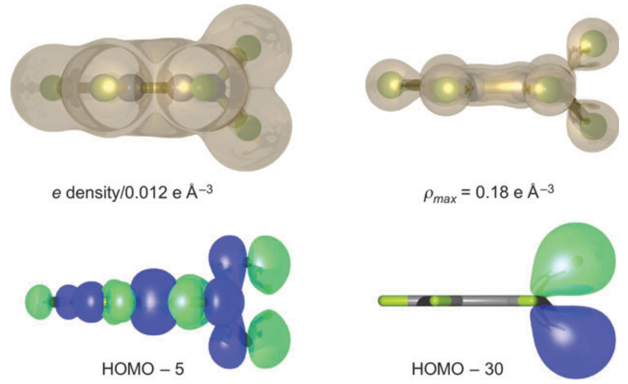

Fig. 11 Graphical evaluation of the wavefunction for the C_6F_6–F^- strong σ complex (Fig. 10). Electron density surfaces are shown at the anion–π limit of 0.012 e Å^{-3} (top, left) and the ρ_{max} value of 0.18 e Å^{-3} (top, right). MOs are rendered at 0.032 (e Å^{-3})$^{1/2}$ isovalues.

quite short, ranging from 1.48 to 1.51 Å, close to the mean value observed for C(sp^3)–F bonds in the CSD, 1.46 ± 0.02 Å.

Though there is little doubt regarding the predominantly covalent nature of this interaction motif, we now present a graphical evaluation of the wavefunction for the C_6F_6–F^- σ complex, both (i) to provide a point of contrast to the prior TAZ–Br^- results (Figs. 5 and 6) and (ii) to illustrate the difference between strongly covalent *versus* weakly covalent (see part (c) below) σ interactions. Plots of electron density and MO isosurfaces for the C_6F_6–F^- complex are given in Fig. 11. At a density of 0.012 e Å^{-3}, where the isosurfaces for anion–π complexes are discontinuous, substantial electron density remains between F^- and the arene. In fact, it is necessary to increase the isosurface value above 0.18 e Å^{-3} before discontinuity is attained for C_6F_6–F^-, consistent with strong covalent bonding. The ρ_{max} values for other arene–F^- σ complexes in our study all surpass 0.15 e Å^{-3}. Thus, these *strong σ interactions* exhibit at least an order of magnitude more electron density between the halide and arene than anion–π interactions.

As anticipated, examination of the MOs in the C_6F_6–F^- σ complex reveals significant and extensive mixing of anion orbitals with arene orbitals. For example, with the exception of HOMO-2, the 10 highest occupied MOs all show blending of the F^- and C_6F_6 orbitals. The bonding MOs shown in Fig. 11 are representative examples that predominantly involve either F^- p orbitals, as in HOMO-5, or F^- s orbitals, as in HOMO-30. This behavior, which is exhibited by all arene–F^- σ complexes that we examined, contrasts sharply with the absence of mixing observed for the anion–π complexes of the Cl^- and Br^- anions.

(c) Weakly covalent σ complexes

As noted in the earlier discussion of anion–π complexes (see part (a) above), a search of the crystal structure database for halides contacting the face of electron-deficient arenes yielded only a handful of examples. In the majority of these data, the halide is located outside the periphery of the π-system (see Fig. 7). Although it might be thought that these cases, such as the examples shown in Fig. 12,[22,61–63] represent anion–π interactions distorted by crystal packing forces, we obtained theoretical evidence for the existence of a third binding motif for the less nucleophilic Cl^- and Br^- anions that exhibits the observed off-center binding geometry.[22] In what follows, we describe the nature of these complexes and offer a rationale for calling this third motif the weakly covalent σ interaction.

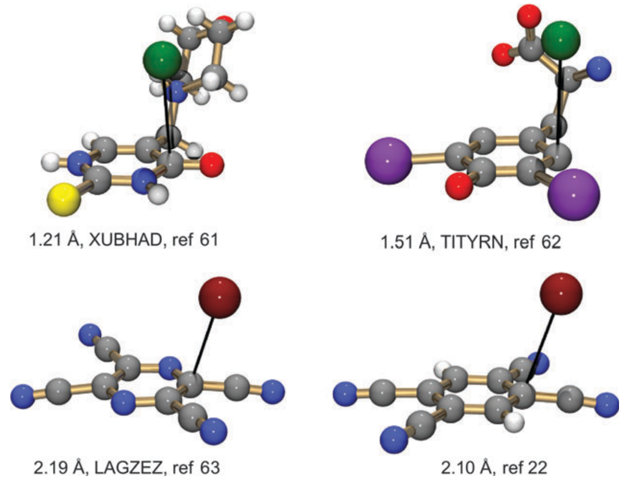

Fig. 12 Examples of crystal structures in which the halide is located above or outside the periphery of the arene ring. Values for d_{offset} (see Fig. 7), the CSD refcode, and reference are given for each structure.

For all arenes investigated except C_6F_6, we located minima for both Cl^- and Br^- in which the halide was located outside the ring periphery.[22] With the halides located 2.6 to 3.1 Å above the mean arene plane, the calculated geometries exhibit d_{offset} values ranging from 1.7 to 2.0 Å. Representative Cl^- geometries are presented in Fig. 13. In the case of Cl^-, this

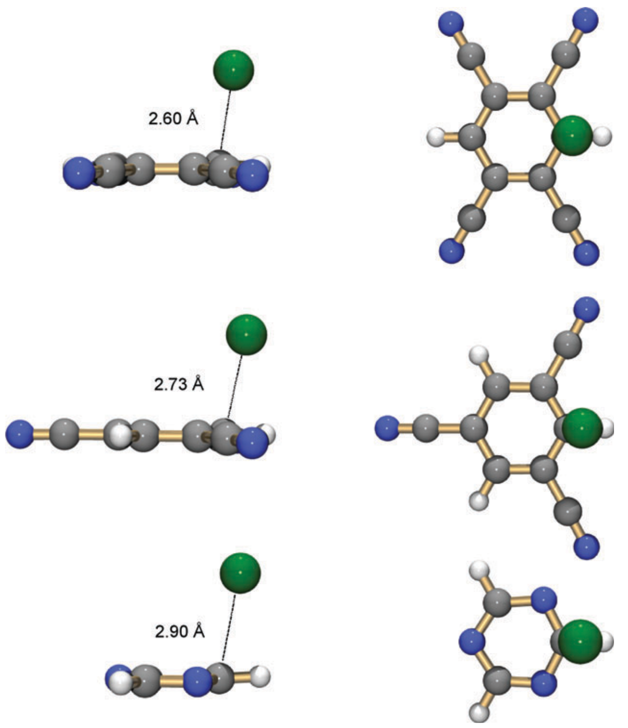

Fig. 13 Examples of weak σ complexes formed between Cl^- and 4CN (top), 3CN (middle), and TAZ (bottom). Geometries were optimized at the MP2/aug-cc-pVDZ level of theory.[22]

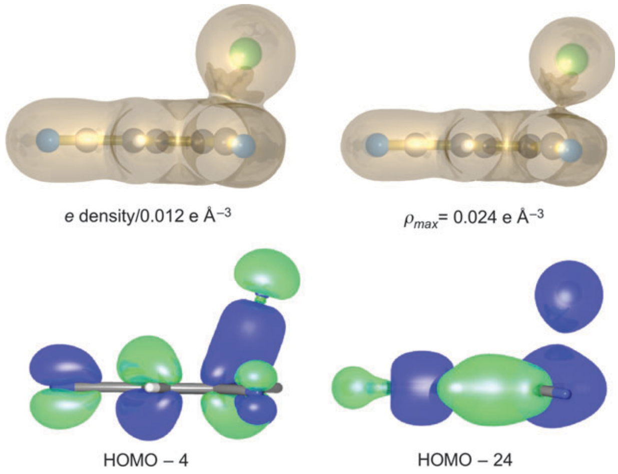

Fig. 14 Graphical evaluation of the wavefunction for the 3CN–Cl$^-$ weak σ complex (Fig. 13). Electron density surfaces are shown at the anion–π limit of 0.012 e Å^{-3} (top, left) and the ρ_{max} value of 0.024 e Å^{-3} (top, right). MOs are rendered at 0.032 (e Å^{-3})$^{1/2}$ isovalues.

off-center binding motif is the only stable geometry for interaction with the π-systems of 3CN and 4CN. With Br$^-$, the same behavior was exhibited by 4CN, but both off-center and anion–π geometries were obtained for 3CN. These were the first reported instances where a halide other than F$^-$ failed to form a stable anion–π complex with an electron-deficient arene. The least electron-deficient arene, TAZ, yielded both off-center and anion–π motifs as minima for Cl$^-$ and Br$^-$.

At first glance, the off-center geometries shown in Fig. 13 bear a much closer resemblance to the strongly covalent σ complexes shown for F$^-$ (Fig. 10) than to the anion–π complexes shown for Br$^-$ (Fig. 4). Further scrutiny reveals some significant differences. Where the F–C distances were approaching the average F–C(sp^3) distance, the Cl–C distances, which range from 2.60 to 2.90 Å, are quite elongated when compared to the 1.78 ± 0.04 Å average Cl–C(sp^3) distance observed in the CSD. As a consequence, the contacted carbon atom retains a trigonal planar geometry, rather than the tetrahedral geometry observed in the F$^-$ complexes.

The geometries of the off-center Cl$^-$ complexes are rationalized by the presence of covalent character that is weaker than that observed for the F$^-$ complexes. Evidence in support of this rationalization is obtained upon graphical analysis of the wavefunctions for these complexes. Plots of electron density and MO isosurfaces for the 3CN–Cl$^-$ complex are given in Fig. 14. At a density of 0.012 e Å^{-3}, where the isosurfaces for anion–π complexes are discontinuous, electron density remains between Cl$^-$ and the arene. Gradually increasing the density value yields a ρ_{max} of 0.024 e Å^{-3}. This value, which lies between the 3CN–Br$^-$ anion–π complex, ρ_{max} = 0.010 e Å^{-3}, and the 3CN–F$^-$ σ complex, ρ_{max} = 0.16 e Å^{-3}, is indicative of a weak covalent bond.

The nature of the bonding interaction is elucidated on inspection of the MOs. In contrast to strong σ interactions, which show extensive blending of anion and arene orbitals in many MOs, only three MOs show significant mixing in this weak σ complex. Two of these are bonding in character. These are HOMO-4, which involves a Cl$^-$ p orbital, and HOMO-24, which involves a Cl$^-$ s orbital (see Fig. 14).

The behavior exhibited by the 3CN–Cl$^-$ example is representative of the complexes that exhibit the off-center geometry. Their ρ_{max} values range from 0.014 e Å^{-3} for TAZ–Br$^-$ up to 0.031 e Å^{-3} for 4CN–Cl$^-$. Despite the long halide–carbon distances, there is electron density transferred from the halide to the arene in bonding MOs involving both s and p halide orbitals. As expected, both the degree of covalency and the strength of the interaction correlate with the halide–carbon distance. For example, the Cl$^-$ complexes shown in Fig. 13 exhibit the following values (arene, Cl–C distance, ρ_{max}, ΔE): 4CN, 2.60 Å, 0.031 e Å^{-3}, −124.7 kJ mol^{-1}; 3CN, 2.73 Å, 0.024 e Å^{-3}, −95.1 kJ mol^{-1}; TAZ, 2.90 Å, 0.015 e Å^{-3}, −36.3 kJ mol^{-1}.

The foregoing analysis establishes that these off-center geometries have a small, but readily detectable, degree of covalent character involving the delocalization of charge from the anion to the arene. Given the different geometry and presence of covalent character, it would be inappropriate to call them anion–π complexes. On the other hand, they do not exhibit the characteristics of strongly covalent σ complexes. Since the covalent interaction is σ in character, in other words, involves orbitals that are symmetric about the bond axis, we propose the nomenclature *weak σ interaction* to refer to this bonding motif.

Existing data suggest that the weak σ motif is the preferred binding mode for the interaction of Cl$^-$, Br$^-$, and I$^-$ with strongly electron-deficient arenes. This statement is supported by the theoretical evidence reviewed herein, which shows weak σ interactions to be the most stable motif for 3CN and 4CN, as well as by experimental studies involving arenes with high electron affinities. Crystal structures have shown that 4CN forms weak σ complexes with Br$^-$ and I$^-$.[22] Analogous behavior was observed with a series of crystal structures of Cl$^-$, Br$^-$, and I$^-$ complexes with the even more electron-deficient arenes, tetracyanopyrazine and tetrachloro-*o*-benzoquinone.[63]

An interesting property of these crystals is that they were highly colored, even though the individual salts and arenes were colorless prior to mixing. Moreover, when halide salts were added to solution containing highly electron-deficient arenes, intense adsorption in the visible region was

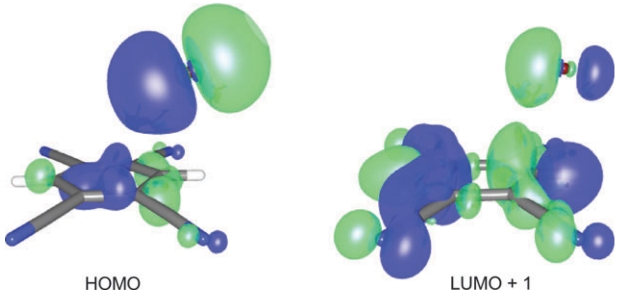

Fig. 15 Donor (HOMO) and acceptor (LUMO + 1) orbitals involved in the visible transition exhibited by the 4CN–Br$^-$ weak σ complex. MOs, obtained at the B3LYP/aug-cc-pVDZ level of theory,‡ are rendered at 0.032 (e Å^{-3})$^{1/2}$ isovalues.

observed.[22,63] Detailed analysis of UV–Vis spectral data established the behavior of these systems to be diagnostic of classic electron donor π-acceptor charge-transfer behavior.[63] In charge-transfer complexes, donors such as Br^- and acceptors such as 4CN interact to form complexes that adsorb light in a manner different from either of the partners. The visible excitation of this complex involves the transfer of an electron from the Br^- donor to the 4CN acceptor. Although the optically induced excited state could, in theory, stabilize the complex by shifting the equilibrium to the right, in practice the excited states are generally high enough in energy that their contribution to the complex stability is small.[1b]

$$Br^- + 4CN \xrightleftharpoons{K} Br^-,4CN \xrightarrow{h\nu} Br,4CN^-$$

To confirm the charge-transfer behavior of the weak σ complexes, we performed time-dependent density functional theory, TDDFT,[64] calculations on the 4CN–Br^- complex, which has an adsorption near 380 nm in CH_3CN.[65] In the absence of Br^-, the arene exhibits intense π to π* transitions in the UV region, but no transitions in the visible range. On the other hand, the weak σ complex exhibits a visible transition involving the transfer of charge from the HOMO, which is predominantly composed of a Br^- p orbital, to the LUMO + 1, which is mainly localized on the arene, as illustrated in Fig. 15. The computed transition energy, 2.68 eV (462 nm), is somewhat lower than the experimental value, 3.26 eV (380 nm). Nevertheless, the calculation qualitatively predicts the presence of a visible charge-transfer band for this complex.

(d) Binding motifs for anions other than halides?

Whereas anion interactions with arene π-systems have been well characterized for halides, less attention has been given to other anions. Theoretical studies have been conducted on a variety of systems, but in most cases attention has remained riveted on the anion–π interaction and information on alternate binding modes remains scarce. A study on perfluoroarenes included MP2 geometries for CN^-, HCC^-, ONC^-, CNO^-, H^-, and CH_3^- anions with C_6F_6, but failed to establish whether these structures were minima on this potential surface.[31] Another study reported MP2 geometries for high symmetry complexes of C_6F_6 with H^-, CN^-, CO_3^{2-}, and NO_3^-, in which that anion was located above the ring centroid.[29] Here, frequency calculations revealed H^- and NO_3^- complexes to be minima, while CN^- and CO_3^{2-} were unstable. Yet a third study at the MP2 level reports high symmetry geometries for C_6F_6 adducts with CN^-, NC^-, NO_3^- and CO_3^{2-}, finding the CN^- and NO_3^- complexes to be minima, while the NC^- and CO_3^{2-} forms were not.[33] In instances where the high symmetry forms were unstable with C_6F_6, all studies noted that the anion attacked the ring to form a σ complex. However, since the focus of these papers was the anion–π interaction, no characterizations of these σ complexes were reported.

In addition to perfluoroarenes, MP2 studies of other anions have been limited to triazines. Anion–π interactions, σ interactions, and "an apparent π–π stacking interaction" were reported for N_3^- complexes with TAZ and 1,3,5-trifluorotriazine.[28] Calculations show that for high symmetry geometries with CN^-, NC^-, NO_3^- and CO_3^{2-} centered above TAZ, the only anion complex found to be a minimum was that of NO_3^-.[33] Recently, high symmetry geometries of BH_4^-, BF_4^-, and PF_6^- have been established as minima for 1,3,5-trifluorotriazine.[45]

With all of the concentration on the anion–π interaction, there is now a tendency to label every structure containing an anion above an arene plane as another example of the anion–π interaction. Based on the behavior of halide complexes, however, it is a reasonable conjecture that other anions also may exhibit more than one binding motif. With halides, the geometry of the noncovalent anion–π complex is characteristic and distinct from the covalent σ forms. The situation is not as clear for non-spherical anions. Labeling an anion–arene contact as an anion–π interaction, in other words, as a noncovalent interaction, without some analysis of the bonding is a questionable practice and possible source of confusion. A recent example of this occurs with TAZ–NO_3^- complexes.

As noted above, earlier MP2 calculations identified a minimum in which NO_3^- was centered above TAZ such that the planes of the two molecules were parallel yielding a C_{3v}

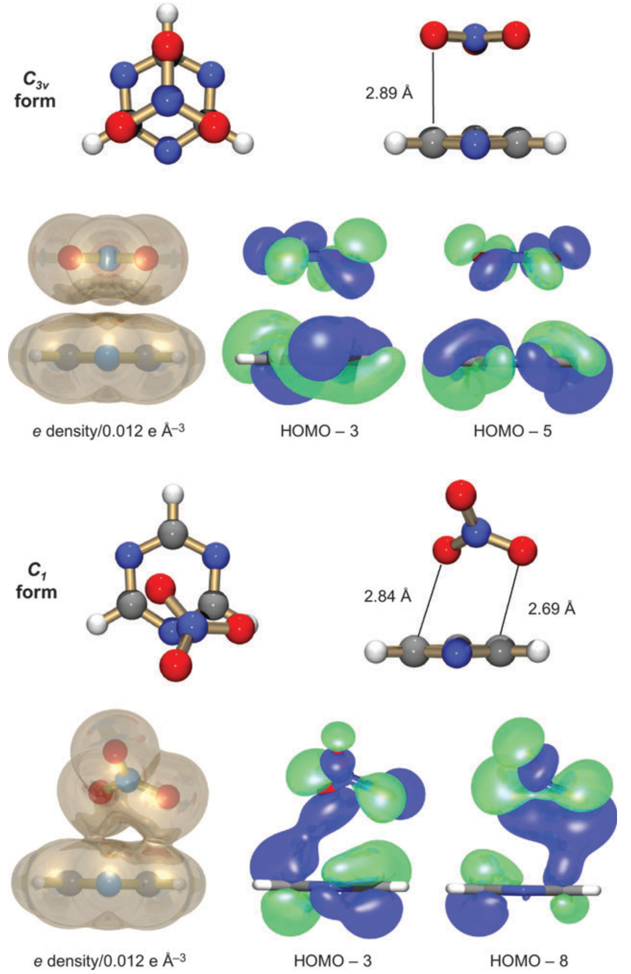

Fig. 16 Optimized geometries, electron density isosurfaces and MOs (0.032 (e Å^{-3})$^{1/2}$) for the C_{3v} symmetric anion–π complex (top) and the C_1 symmetric weak σ complex (bottom). Calculations performed at the MP2/aug-cc-pVDZ level of theory.‡

symmetric geometry. This geometry was declared to be an anion–π complex.[33] Recently, a quite different orientation was observed in several crystal structures for NO_3^- interacting with a 1,3,5-alkyl-substituted triazine ring.[42,43] Geometry optimizations using DFT[42] and MP2[43] methods yielded an asymmetric geometry, in other words, with C_1 symmetry, for a complex of NO_3^- with TAZ. This geometry, which was slightly more stable than the C_{3v} form, also was declared to be an anion–π complex.

To clarify the nature of these interactions, we have repeated the calculations at the MP2/aug-cc-pVDZ level of theory, locating both the C_{3v} and C_1 geometries as minima, and evaluated the extent of covalency using the graphic methods as presented above. The results are summarized in Fig. 16. Although the C_{3v} form does exhibit some blending of MOs between NO_3^- and TAZ, this symmetric structure exhibits ρ_{max} = 0.011 e Å^{-3}, below the 0.012 e Å^{-3} limit established for halide anion–π complexes. The C_1 form, however, exhibits ρ_{max} = 0.014 e Å^{-3}, the same as the values of 0.014 and 0.015 e Å^{-3} observed for the weakly covalent σ complexes that TAZ forms with Br^- and Cl^-, respectively. Representative MOs for the C_1 complex show significantly more mixing than in the C_{3v} case, consistent with the presence of more covalent character. As with the halides, it is this additional covalent bonding that results in the asymmetric geometry of the complex. Thus, reasoning by analogy with halide behavior, the C_{3v} form is an example of an anion–π interaction whereas the C_1 form is actually an example of a weak σ interaction. The ΔE values for these complexes, −46.2 kJ mol^{-1} for the anion–π complex *versus* −49.5 kJ mol^{-1} for the weak σ complex, mimic the previously reported DFT stability difference of 2.3 kJ mol^{-1}.[42]

Summary

If the relative importance of an interaction can be judged by the frequency of its occurrence in the solid-state, then by far the most important anion–arene interaction is C–H hydrogen bonding. There are thousands of examples in the CSD. Even in the absence of electron-withdrawing substituents, aryl C–H groups form hydrogen bonds with anions that are comparable in strength to more conventional N–H and O–H donors. The strength of this interaction can be moderated by arene substitution, allowing donor group strength to be tuned.

Addition of electron-withdrawing substituents can produce strong hydrogen bonds, with anion binding strengths in excess of −100 kJ mol^{-1}. Despite their potential use as binding sites in anion receptors, few host architectures have been designed deliberately to use charge-neutral arenes as hydrogen bond donors.[21,66] Further exploitation of this motif in ligand design is warranted.

Although the interactions are comparable in stability with aryl C–H hydrogen bonding, the CSD offers only a handful of examples for anion interactions with π-systems of charge-neutral arenes. Three distinct modes of binding, distinguished by their geometric features as well as by their degree of covalency, have been characterized by electronic structure calculations. The preferred π-system binding mode depends on the nature of the anion and the arene. It is possible to suggest some rough guidelines for which binding modes will be observed as minima in calculations on 1 : 1 arene–anion complexes.

Strong σ complexes are most likely with nucleophilic anions such as RO^-, CN^-, and F^- with any electron-deficient arene. Anion–π complexes are most likely with large, charge-diffuse anions such as ClO_4^-, BF_4^-, and PF_6^- with arenes of moderate electron affinity. Results on more charge-dense anions such as Cl^-, Br^-, and NO_3^- have shown that both weak σ and anion–π complexes can occur with arenes of moderate electron affinity, such as TAZ. However, as the electron affinity of the arene is increased, anion–π complexes become unstable and weak σ complexes are favored. Although there have been several anion receptor designs that make use of anion–π interaction,[39,44,55,66,67] there have been no reports of host architectures designed to take advantage of the weak σ interaction. We note that the presence of visible charge-transfer adsorption bands raises the possibility of exploiting the weak σ motif in the design of colorimetric anion sensors.

When aryl C–H groups are present, there is the possibility of competition between C–H bonding *versus* π-system bonding. For arenes with moderate electron affinity, such as TAZ[22,28] and C_6F_5H,[68] C–H hydrogen bonding yields a stronger complex with Cl^- than interactions with the π-system. This situation is reversed with strongly electron-deficient arenes, such as 3CN and 4CN, where the weak σ interactions are stronger than the C–H hydrogen bond interactions.[22]

Whereas anion–arene interactions have been characterized extensively for halides, fewer data are available for other anions. Given the possibility of different binding motifs, observation of an anion above the plane of an electron-deficient arene is necessary, but not sufficient, evidence for an anion–π interaction. It is also necessary to establish that the interaction is noncovalent. In this review, we have shown how graphical rendering of electron density and MO isosurfaces provides an informative tool for visualizing the degree of covalency. We also have demonstrated how electron density isosurfaces provide one quantitative measure of covalent character, ρ_{max}, that can be used to classify the binding motif. Because the degree of covalency can vary continuously from purely noncovalent to purely covalent, the definition of what is meant by noncovalent is somewhat arbitrary. Based on the behavior of the systems we have examined thus far, we propose the following tentative scale at the MP2/aug-cc-pVDZ level of theory: noncovalent anion–π interaction, ρ_{max} <0.012 e Å^{-3}, weakly covalent σ interaction 0.012 ≤ ρ_{max} ≤ 0.100 e Å^{-3}, and strongly covalent σ interaction, ρ_{max} >0.10 e Å^{-3}.

---

‡ Electronic structure calculations were carried out with the NWChem program[69] using second order Møller–Plesset perturbation theory (MP2).[70]

Geometries were optimized using the augmented correlation consistent double-ζ basis set (aug-cc-pVDZ)[71] and frozen core approximation in the correlation treatment. Frequency calculations were performed at the same level of theory to characterize each stationary point as a minimum or a transition state. TDDFT calculations were performed with the TURBOMOLE program.[72] Structures were re-optimized at the B3LYP/aug-cc-pVDZ level using TURBOMOLE's JOBEX program[73] and low-lying singlet excitation energies and intensities were computed at the TDDFT level using the ESCF module.[74,75] Electron density and MO isosurfaces were rendered with ECCE.[47]

The following statement regarding the interaction of anions with arenes, made some time ago, continues to provide an accurate synopsis of the character of anion–arene interactions: "Depending on the nature of the substituents and X^- an interesting variety of most stable structures can occur."[3b] As noted in this prior paper and as we have seen herein, this interesting variety includes C–H hydrogen bonding, anion–π, and a range of σ interactions. Although both gas phase measurements and calculated ΔE ranges indicate that the stabilities of these binding motifs are comparable, the supramolecular community has focused on the anion–π interaction, largely ignoring the existence of other motifs. Similarly, the theory community has reported a large number of symmetric anion–π geometries, but for the most part has neglected to characterize the alternate, stable interaction motifs likely present in many anion–arene systems studied. Perhaps it is time to broaden our perspective.

Acknowledgements

B.P.H. acknowledges support from the Division of Chemical Sciences, Geosciences, and Biosciences, Office of Basic Energy Sciences, US Department of Energy (DOE) under contract number DE-AC05-00OR22725 with Oak Ridge National Laboratory (managed by UT-Battelle, LLC). MP2 calculations were performed using the Molecular Science Computing Facility (MSCF) in the William R. Wiley Environmental Molecular Sciences Laboratory, a national scientific user facility sponsored by the DOE's Office of Biological and Environmental Research and located at Pacific Northwest National Laboratory, managed for DOE by Battelle. TDDFT calculations were performed using the computing facilities of the Materials and Process Simulation Center at the California Institute of Technology, supported by grants from ARO-DURIP, ONR-DURIP, and NSF-MRI.

Notes and references

1 For reviews on charge-transfer complexes see: (*a*) J. N. Murrell, *Q. Rev. Chem. Soc.*, 1961, **15**, 191; (*b*) E. Kosower, *Prog. Phys. Org. Chem.*, 1965, **3**, 81; (*c*) J. Rose, *Molecular Complexes*, Pergamon, New York, NY, 1967.

2 For reviews on nucleophilic aromatic substitution see: (*a*) E. Buncel, A. R. Norris and K. E. Russell, *Q. Rev. Chem. Soc.*, 1968, **22**, 123; (*b*) M. J. Strauss, *Chem. Rev.*, 1970, **70**, 667; (*c*) G. A. Artamkina, M. P. Egorov and I. P. Beletskaya, *Chem. Rev.*, 1982, **82**, 427; (*d*) F. Terrier, *Chem. Rev.*, 1982, **82**, 77; (*e*) E. Buncel, J. M. Dust and F. Terrier, *Chem. Rev.*, 1995, **95**, 2262.

3 (*a*) P. Kebarle and S. Chowdhury, *Chem. Rev.*, 1987, **87**, 513; (*b*) G. J. C. Paul and P. Kebarle, *J. Am. Chem. Soc.*, 1991, **113**, 1148.

4 *Supramolecular Chemistry of Anions*, ed. A. Bianchi, K. Bowman-James and E. García-España, Wiley-VCH, New York, NY, 1997.

5 (*a*) F. P. Schmidtchen and M. Berger, *Chem. Rev.*, 1997, **97**, 1609; (*b*) P. A. Gale, *Coord. Chem. Rev.*, 2000, **199**, 181; (*c*) P. A. Gale, *Coord. Chem. Rev.*, 2001, **213**, 79; (*d*) P. D. Beer and P. A. Gale, *Angew. Chem., Int. Ed.*, 2001, **40**, 486; (*e*) R. J. Fitzmaurice, G. M. Kyne, D. Douheret and J. D. Kilburn, *J. Chem. Soc., Perkin Trans. 1*, 2002, 841; (*f*) R. Martínez-Máñez and F. Sacenón, *Chem. Rev.*, 2003, **103**, 4419; (*g*) C. Suksai and T. Tuntulani, *Chem. Soc. Rev.*, 2003, **32**, 192; (*h*) K. Choi and A. D. Hamilton, *Coord. Chem. Rev.*, 2003, **240**, 101; (*i*) T. N. Lambert and B. D. Smith, *Coord. Chem. Rev.*, 2003, **240**, 129; (*j*) A. P. Davis and J.-B. Joos, *Coord. Chem. Rev.*, 2003, **240**, 143; (*k*) P. A. Gale, *Coord. Chem. Rev.*, 2003, **240**, 191; (*l*) *Fundamentals and Applications of Anion Separations*, ed. B. A. Moyer and R. P. Singh, Kluwer Academic/Plenum, New York, NY, 2004; (*m*) O. N. Chupakhin, N. A. Itsikson, Y. Y. Morzherin and V. N. Charushin, *Heterocycles*, 2005, **66**, 689; (*n*) S. Kubik, C. Reyheller and S. Stüwe, *J. Inclusion Phenom. Macrocycl. Chem.*, 2005, **52**, 137; (*o*) F. P. Schmidtchen, *Top. Curr. Chem.*, 2005, **255**, 1; (*p*) P. A. Gale, *Acc. Chem. Res.*, 2005, **39**, 465; (*q*) M. H. Filby and J. W. Steed, *Coord. Chem. Rev.*, 2006, **250**, 3200; (*r*) J. W. Steed, *Chem. Commun.*, 2006, 2637; (*s*) E. A. Katayev, Y. A. Ustynyuk and J. L. Sessler, *Coord. Chem. Rev.*, 2006, **250**, 2004; (*t*) C. Schmuck, *Coord. Chem. Rev.*, 2006, **250**, 3053; (*u*) A. P. Davis, D. N. Sheppard and B. D. Smith, *Chem. Soc. Rev.*, 2007, **36**, 348; (*v*) P. A. Gale, S. E. García-Garrido and J. Garric, *Chem. Soc. Rev.*, 2008, **37**, 151; (*w*) C.-H. Lee, H. Miyaji, D.-W. Yoon and J. L. Sessler, *Chem. Commun.*, 2008, 24.

6 (*a*) B. P. Hay, D. A. Dixon, J. C. Bryan and B. A. Moyer, *J. Am. Chem. Soc.*, 2002, **124**, 182; (*b*) B. P. Hay, M. Gutowski, D. A. Dixon, J. Garza, R. Vargas and B. A. Moyer, *J. Am. Chem. Soc.*, 2004, **126**, 7925; (*c*) B. P. Hay, T. K. Firman and B. A. Moyer, *J. Am. Chem. Soc.*, 2005, **127**, 1810.

7 V. S. Bryantsev and B. P. Hay, *J. Am. Chem. Soc.*, 2006, **128**, 2035.

8 For recent overviews see: (*a*) P. Gamez, T. J. Mooibroek, S. J. Teat and J. Reedijk, *Acc. Chem. Res.*, 2007, **40**, 435; (*b*) B. L. Schottel, H. T. Chifotides and K. R. Dunbar, *Chem. Soc. Rev.*, 2008, **37**, 68.

9 (*a*) I. Alkorta and J. Elguero, *J. Phys. Chem. A*, 2003, **107**, 9428; (*b*) C. Garau, A. Frontera, D. Quiñonero, P. Ballester, A. Costa and P. M. Deya, *Chem. Phys. Lett.*, 2003, **382**, 534; (*c*) C. Garau, D. Quiñonero, A. Frontera, P. Ballester, A. Costa and P. M. Deya, *New J. Chem.*, 2003, **370**, 7; (*d*) R. M. Fairchild and K. T. Holman, *J. Am. Chem. Soc.*, 2005, **127**, 16364; (*e*) B. L. Schottel, J. Bacsa and K. R. Dunbar, *Chem. Commun.*, 2005, 46; (*f*) B. L. Schottel, H. T. Chifotides, M. Shatruk, A. Chouai, L. M. Perez, J. Bacsa and K. R. Dunbar, *J. Am. Chem. Soc.*, 2006, **128**, 5895; (*g*) C. A. Black, L. R. Hanton and M. D. Spicer, *Chem. Commun.*, 2007, 3171; (*h*) J. T. Lenthall and J. W. Steed, *Coord. Chem. Rev.*, 2007, **251**, 1747.

10 D. Quiñonero, A. Frontera, D. Escudero, P. Ballester, A. Costa and P. M. Deya, *ChemPhysChem*, 2007, **8**, 1182.

11 G. R. Desiraju and T. Steiner, *The Weak Hydrogen Bond in Structural Chemistry and Biology*, Oxford University Press, New York, NY, 1999.

12 G. A. Jeffrey, *An Introduction to Hydrogen Bonding*, Oxford University Press, New York, NY, 1997.

13 R. Vargas, J. Garza, D. A. Dixon and B. P. Hay, *J. Am. Chem. Soc.*, 2000, **122**, 4750.

14 M. W. Feyereisen, D. Feller and D. A. Dixon, *J. Phys. Chem.*, 1996, **100**, 2993.

15 D. A. Dixon, K. D. Dobbs and J. J. Valentini, *J. Phys. Chem.*, 1994, **98**, 13435.

16 M. A. French, S. Ikuta and P. Kebarle, *Can. J. Chem.*, 1982, **60**, 1907.

17 J. W. Larson and T. B. McMahon, *J. Am. Chem. Soc.*, 1984, **106**, 517.

18 K. Hiraoka, S. Mizuse and S. Yamabe, *Chem. Phys. Lett.*, 1988, **147**, 174.

19 Z. M. Loh, R. L. Wilson, D. A. Wild and E. J. Bieske, *J. Chem. Phys.*, 2003, **119**, 9559.

20 V. S. Bryantsev and B. P. Hay, *J. Am. Chem. Soc.*, 2005, **127**, 8282.

21 V. S. Bryantsev and B. P. Hay, *Org. Lett.*, 2005, **7**, 5031.

22 O. B. Berryman, V. S. Bryantsev, D. P. Stay, D. W. Johnson and B. P. Hay, *J. Am. Chem. Soc.*, 2007, **129**, 48.

23 F. H. Allen, *Acta Crystallogr., Sect. B: Struct. Sci.*, 2002, **58**, 380.

24 (*a*) S. K. Mandal and A. R. Chakravarty, *Polyhedron*, 1992, **11**, 823; (*b*) M. K. Denk, S. Gupta and A. J. Lough, *Eur. J. Inorg. Chem.*, 1999, 41.

25 (*a*) T. Kohler, D. Seidel, V. Lynch, F. O. Arp, Z. Ou, K. M. Kadish and J. L. Sessler, *J. Am. Chem. Soc.*, 2003, **125**, 6872; (*b*) S. D. Drouin, S. Monfette, D. Amoroso, G. P. A. Yap and D. E. Fogg, *Organometallics*, 2005, **24**, 4721.

26 S. Chowdhury and P. Kebarle, *J. Chem. Phys.*, 1986, **85**, 4989.

27 K. Hiraoka, S. Mizuse and S. Yamabe, *J. Phys. Chem.*, 1987, **91**, 5294.

28 M. Mascal, A. Armstrong and M. D. Bartberger, *J. Am. Chem. Soc.*, 2002, **124**, 6247.
29 D. Quiñonero, C. Garau, C. Rotger, A. Frontera, P. Ballester, A. Costa and P. M. Deyà, *Angew. Chem., Int. Ed.*, 2002, **41**, 3389.
30 D. Quiñonero, C. Garau, A. Frontera, P. Ballester, A. Costa and P. M. Deyà, *Chem. Phys. Lett.*, 2002, **359**, 486.
31 I. Alkorta, I. Rozas and J. Elguero, *J. Am. Chem. Soc.*, 2002, **124**, 8593.
32 (*a*) D. A. Dougherty, *Science*, 1993, **261**, 5129; (*b*) J. C. Ma and D. A. Dougherty, *Chem. Rev.*, 1997, **97**, 1303.
33 D. Kim, P. Tarakeshwar and K. S. Kim, *J. Phys. Chem. A*, 2004, **108**, 1250.
34 C. Garau, A. Frontera, D. Quiñonero, P. Ballester, A. Costa and P. M. Deyà, *J. Phys. Chem. A*, 2004, **108**, 9423.
35 C. Garau, A. Frontera, D. Quiñonero, P. Ballester, A. Costa and P. M. Deyà, *Chem. Phys. Lett.*, 2004, **392**, 85.
36 D. Quiñonero, C. Garau, A. Frontera, P. Ballester, A. Costa and P. M. Deyà, *J. Phys. Chem. A*, 2005, **109**, 4632.
37 C. Garau, A. Frontera, P. Ballester, D. Quiñonero, A. Costa and P. M. Deyà, *Eur. J. Org. Chem.*, 2005, 179.
38 C. Garau, D. Quiñonero, A. Frontera, P. Ballester, A. Costa and P. M. Deyà, *J. Phys. Chem. A*, 2005, **109**, 9341.
39 A. Frontera, F. Saczewski, M. Gdaniec, E. Dziemidowicz-Borys, A. Kurland, P. M. Deyà, D. Quiñonero and C. Garau, *Chem.–Eur. J.*, 2005, **11**, 6560.
40 D. Quiñonero, A. Frontera, C. Garau, P. Ballester, A. Costa and P. M. Deya, *ChemPhysChem*, 2006, **7**, 2487.
41 A. Clements and M. J. Lewis, *J. Phys. Chem. A*, 2006, **110**, 12705.
42 H. Casellas, C. Massera, F. Buda, P. Gamez and J. Reedijk, *New J. Chem.*, 2006, **30**, 1561.
43 P. U. Maheswari, B. Modec, A. Pevec, B. Kozlevcar, C. Massera, P. Gamez and J. Reedijk, *Inorg. Chem.*, 2006, **45**, 6637.
44 M. Mascal, *Angew. Chem., Int. Ed.*, 2006, **45**, 2890.
45 C. Garau, D. Quiñonero, A. Frontera, D. Escudero, P. Ballester, A. Costa and P. M. Deya, *Chem. Phys. Lett.*, 2007, **438**, 104.
46 A. Frontera, D. Quiñonero, A. Costa, P. Ballester and P. M. Deya, *New J. Chem.*, 2007, **31**, 556.
47 G. Black, J. Daily, B. Didier, T. Elsethagen, D. Feller, D. Gracio, M. Hackler, S. Havre, D. Jones, E. Jurrus, T. Keller, C. Lansing, S. Matsumoto, B. Palmer, M. Peterson, K. Schuchardt, E. Stephan, L. Sun, K. Swanson, H. Taylor, G. Thomas, E. Vorpagel, T. Windus and C. Winters, *ECCE, A Problem Solving Environment for Computational Chemistry, Software Version 4.5*, Pacific Northwest National Laboratory, Richland, Washington 99352-0099, USA, 2007.
48 W. J. Hehre, *A Guide to Molecular Mechanics and Quantum Chemical Calculations*, Wavefunction, Irvine, CA, 2003.
49 R. F. W. Bader, *Atoms in Molecules, A Quantum Theory*, Oxford University Press, New York, NY, 1990.
50 J. Stewart, I. Katsuyama, H. Fahmy, F. R. Fronczek and J. K. Zjawiony, *Synth. Commun.*, 2004, **34**, 547.
51 V. Cody and P. A. Sutton, *Anti-Cancer Drug Des.*, 1987, **2**, 253.
52 L.-C. Yu, H. Liang, C.-S. Zhou, Z.-F. Chen and Y. Zhang, *Acta Crystallogr., Sect. E*, 2004, **60**, o1051.
53 S. Demeshko, S. Dechert and F. Meyer, *J. Am. Chem. Soc.*, 2004, **126**, 4508.
54 S. Shimizu, R. Taniguchi and A. Osuka, *Angew. Chem., Int. Ed.*, 2005, **44**, 2225.
55 M. Mascal, H. Yakovlev, E. B. Nikitin and J. C. Fettinger, *Angew. Chem., Int. Ed.*, 2007, **46**, 8782.
56 J. March, *Advanced Organic Chemistry, Reactions, Mechanisms, and Structures*, McGraw Hill, New York, NY, 2nd edn, 1977.
57 J. Meisenheimer, *Justus Liebigs Ann. Chem.*, 1902, **323**, 205.
58 R. Destro, T. Pilati and M. Simonetta, *Acta Crystallogr., Sect. B: Struct. Crystallogr. Cryst. Chem.*, 1979, **35**, 733.
59 K. Hiraoka, S. Mizuse and S. Yamabe, *J. Chem. Phys.*, 1987, **86**, 4102.
60 G. W. Dillow and P. Kebarle, *J. Am. Chem. Soc.*, 1988, **110**, 4878.
61 P. Kamalakannan, D. Venkappayya and T. Balasubramanian, *J. Chem. Soc., Dalton Trans.*, 2002, 3381.
62 A. Camerman and N. Camerman, *Acta Crystallogr., Sect. B: Struct. Crystallogr. Cryst. Chem.*, 1974, **30**, 1832.
63 Y. S. Rosokha, S. V. Lindeman, S. V. Rosokha and J. K. Kochi, *Angew. Chem., Int. Ed.*, 2004, **43**, 4650.
64 (*a*) E. Runge and E. K. U. Gross, *Phys. Rev. Lett.*, 1984, **52**, 997; (*b*) E. K. U. Gross and W. Kohn, *Adv. Quantum Chem.*, 1990, **21**, 255; (*c*) M. Petersilka, U. J. Grossmann and E. K. U. Gross, *Phys. Rev. Lett.*, 1996, **76**, 1212.
65 Personal communication with O. B. Berryman, University of Oregon.
66 C.-S. Zuo, J.-M. Quan and Y.-D. Wu, *Org. Lett.*, 2007, **9**, 4219.
67 (*a*) J. M. Hermida-Ramon and C. M. Estevez, *Chem.–Eur. J.*, 2007, **13**, 4743; (*b*) O. B. Berryman, F. Hof, M. J. Hynes and D. W. Johnson, *Chem. Commun.*, 2005, 506.
68 H. Schneider, K. M. Vogelhuber, F. Schinie and J. M. Weber, *J. Am. Chem. Soc.*, 2007, **129**, 13022.
69 E. J. Bylaska, W. A. de Jong, K. Kowalski, T. P. Straatsma, M. Valiev, D. Wang, E. Apra, T. L. Windus, S. Hirata, M. T. Hackler, Y. Zhao, P.-D. Fan, R. J. Harrison, M. Dupuis, D. M. A. Smith, J. Nieplocha, V. Tipparaju, M. Krishnan, A. A. Auer, M. Nooijen, E. Brown, G. Cisneros, G. I. Fann, H. Fruchtl, J. Garza, K. Hirao, R. Kendall, J. A. Nichols, K. Tsemekhman, K. Wolinski, J. Anchell, D. Bernholdt, P. Borowski, T. Clark, D. Clerc, H. Dachsel, M. Deegan, K. Dyall, D. Elwood, E. Glendening, M. Gutowski, A. Hess, J. Jaffe, B. Johnson, J. Ju, R. Kobayashi, R. Kutteh, Z. Lin, R. Littlefield, X. Long, B. Meng, T. Nakajima, S. Niu, L. Pollack, M. Rosing, G. Sandrone, M. Stave, H. Taylor, G. Thomas, J. van Lenthe, A. Wong and Z. Zhang, *NWChem, A Computational Chemistry Package for Parallel Computers, Version 5.0*, Pacific Northwest National Laboratory, Richland, Washington 99352-0999, USA, 2006.
70 C. Möller and M. S. Plesset, *Phys. Rev.*, 1934, **46**, 618.
71 (*a*) T. H. Dunning, Jr, *J. Chem. Phys.*, 1989, **90**, 1007; (*b*) R. A. Kendall, T. H. Dunning, Jr and R. J. Harrison, *J. Chem. Phys.*, 1992, **96**, 6796.
72 R. Ahlrichs, M. Bär, H. P. Baron, R. Bauernschmitt, S. Böcker, P. Deglmann, M. Ehrig, K. Eichkorn, S. Elliott, F. Furche, F. Haase, M. Häser, H. Horn, C. Hättig, C. Huber, U. Huniar, M. Kattannek, A. Köhn, C. Kölmel, M. Kollwitz, K. May, C. Ochsenfeld, H. Öhm, H. Patzelt, O. Rubner, A. Schäfer, U. Schneider, M. Sierka, O. Treutler, B. Unterreiner, M. von Arnim, F. Weigend, P. Weis and H. Weiss, *TURBOMOLE V5-7*, Quantum Chemistry Group, University of Karlsruhe, Karlsruhe, Germany, 2004.
73 M. von Arnim and M. Ahlrichs, *J. Chem. Phys.*, 1999, **111**, 9183.
74 F. Furhe, *J. Chem. Phys.*, 2001, **114**, 5982.
75 F. Furhe and M. Ahlrichs, *J. Chem. Phys.*, 2002, **117**, 7433.